

## Implementation of the Capability of Synchrotron Radiation in a Study of Detonation Processes

E. R. Prueel<sup>a, d</sup>, K. A. Ten<sup>a, d</sup>, B. P. Tolochko<sup>c</sup>, L. A. Merzhievskii<sup>a, d, \*</sup>, L. A. Luk'yanchikov<sup>a, d</sup>,  
V. M. Aul'chenko<sup>b</sup>, V. V. Zhulanov<sup>b</sup>, L. I. Shekhtman<sup>b</sup>, and Academician V. M. Titov<sup>a, d</sup>

Received September 17, 2012

DOI: 10.1134/S1028335813010035

Modern detonation theory is based on the gas-dynamic model developed by Ya.B. Zeldovich, J. von Neumann, and W. Doring. In addition to it, the reaction zone sizes and Neumann peak have been experimentally studied and simulated, the phenomenological kinetics of the detonation transformation has been constructed, attempts to describe the reaction zone by molecular dynamics methods have been undertaken, the data on unloading adiabats have been obtained, numerous equations of state of detonation products have been constructed, and the actual curvature of the detonation front and a number of other properties of the process have been considered. At the same time, there are new facts not complying with the commonly accepted notions and requiring experimental studies and subsequent explanations. Among the actively studied problems are the features of the fine structure of the reaction zone, the Chapman–Jouguet surface shape, the carbon condensation kinetics during the detonation transition, the possibility of transition without a chemical peak, and a number of other problems. Their solution is complicated by the absence of adequate experimental techniques, since the available ones are often perturbative or do not provide spatial and temporal resolution sufficient for unambiguous interpretation. Partial answers to some of these questions can be obtained using the technique

developed and implemented by the authors, based on the use of the soft X-ray component of synchrotron radiation (SR).

Synchrotron radiation is widely used in physics of high energy densities. The prospects of its applications as a tool for studies in this field were analyzed in detail in [1]. Currently, a significant part of predicted techniques has been implemented. A number of reviews and monographs devoted to consideration of the capability and the results of applying SR in various fields of science have been published. A generalized real-time description of the methods for analyzing physical and chemical processes is given, e.g., in [2]. In [3], it was proposed for the first time to use SR as a version of X-ray diffraction methods for studying detonation and shock-wave processes. In comparison with similar conventional methods in which radiation is generated using X-ray tubes, SR has a number of advantages, i.e., high photon flux intensities,  $\sim 10^6$  mm<sup>-2</sup> per exposure, small angular divergence, high stability, and periodicity of radiation bursts (the exposure time is  $\sim 1$  ns and the pulse repetition period is 125 ns). An SR probe beam 20 mm wide and 0.1 mm thick is generated by the develop testbed.

The unique SR properties allow the development of nonperturbative internal methods for studying the parameters of a detonating explosive charge in the region adjacent to the detonation front, including the front itself under certain conditions. We can distinguish three main components of radiation penetrating through the object under study, i.e., those transmitted and deflecting by small and large enough angles. The transmitted beam has the highest intensity and carries information on changes in the material density. The beams deflected by small angles carry information on the density fluctuation in the measurement region. Their intensity is lower by several orders of magnitude. The third type of beams, i.e., diffracted radiation, has an even lower intensity and carries information on the parameters of periodic structures in the material. The

<sup>a</sup> Lavrentyev Institute of Hydrodynamics, Siberian Branch, Russian Academy of Sciences, pr. Akademika Lavrent'eva 15, Novosibirsk, 630090 Russia

<sup>b</sup> Budker Institute of Nuclear Physics, Siberian Branch, Russian Academy of Sciences, pr. Akad. Lavrent'eva 11, Novosibirsk, 630090 Russia

<sup>c</sup> Institute of Solid State Chemistry and Mechanochemistry, Siberian Branch, Russian Academy of Sciences, ul. Kutateladze 18, Novosibirsk, 630128 Russia

<sup>d</sup> Novosibirsk State University, ul. Pirogova 2, Novosibirsk, 630090 Russia

\*e-mail: merzh@hydro.nsc.ru

first two components were used in the methods implemented.

The short time of the processes under study required the development of corresponding measurement methods. The most important element of the measurement system is a DIMEX linear X-ray detector [4] specially developed for dynamic experiments, which makes it possible to record the density distribution of the X-ray flux for a time shorter than the pulse separation; the detector operates with 512 channels each 0.1 mm wide. The electronic circuit of the detector provides storage of information on 32 time points.

### DENSITY MEASUREMENTS IN THE DETONATION WAVE FRONT

These measurements do not yield fundamentally new information; we consider them as a method for testing the technique with the purpose of its possible further application (with improved resolution) to study of the fine structure of the detonation transition zone. To measure the density in the detonation wave front, an explosive charge was placed so that the plane of the formed SR beam would pass through the axis of the charge under study. The SR beam was 20 mm wide and 0.1 mm thick. The detonation front moving with a constant velocity was in the measurement region for several microseconds. The pulse separation was 250 or 500 ns, which allowed 3–5 photographs of the distribution of transmitted radiation by the detector positioned in parallel to the charge axis at a distance of ~1 m. The conditions of such experiments are described in detail in [5]. The material mass in the beam path was determined by the degree of attenuation of radiation passed through the sample as

$$m = \int \rho dL;$$

where  $L$  is the beam path in the charge and  $\rho$  is the instant density at beam points. Independent calibration of the detector was used, based on X-raying of homogeneous plates of the explosive under study [5]. When processing the recorded signal and transforming it to the dependence  $\rho(z)$  (the density distribution

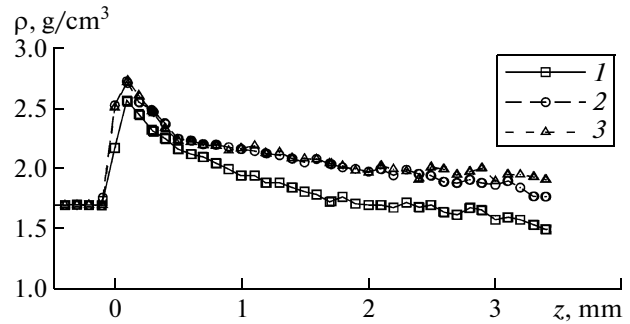


Fig. 1. Density distribution along the charge axis for TH50/50.  $d = (1) 7, (2) 10,$  and  $(3) 12.5$  mm.

along the charge axis), the obtained data were corrected taking into account the signal spread over detector channels and the curvature of the actual detonation wave front [5].

The obtained density distribution along the axis of the trotyl–hexogen (TH) alloy (50/50) charges of various diameters is shown in Fig. 1. These data allow the determination of the state parameters in the Neumann peak and Chapman–Jouguet plane; in the latter case, this is the state at the crossing point of curve portions corresponding to self-similar unloading waves. A comparison showed good agreement of the obtained results with published data. In addition to TH, measurements for trotyl, hexogen, triaminotrinitrobenzene (TATB), TATB-based plasticized composition (PST), and an emulsion explosive (EE) based on ammonium nitrate were performed. The complete data on the parameters at the detonation front of the studied explosives are given in the table. Here  $\rho_0, \rho_N, \rho_{cj}$  are the initial explosive density, the density at the Neumann maximum and in the Chapman–Jouguet, respectively,  $\tau$  and  $\Delta$  are the Neumann peak duration and width,  $\gamma$  is the calculated polytropic exponent of products in the Chapman–Jouguet plane. The column  $\Delta_1$  shows the generalized data on the chemical transformation zone sizes, obtained by various methods, a sufficiently complete list of which is given in [6–8]. The parameter  $K$  introduced in [8] characterizes the ratio of pressures in

Table

Explosive	$\rho_0, \text{g/cm}^3$	$D, \text{km/s}$	$\rho_N, \text{g/cm}^3$	$\rho_{cj}, \text{g/cm}^3$	$\tau, \mu\text{s}$	$\Delta, \text{mm}$	$\Delta_1, \text{mm}$	$\gamma$	$K$
TH	1.7	7.5	2.64	2.16	$0.065 \pm 0.013$	$0.5 \pm 0.1$	0.1–0.8	3	1.81
THT	1.65	6.9	2.61	2.09	$0.1 \pm 0.014$	$0.7 \pm 0.1$	0.63–2.2	3.3	2.09
RDX	1.8	8.6	2.6	2.26	$0.048 \pm 0.012$	$0.4 \pm 0.1$	0.36–0.6	3.1	1.54
TATB	1.8	7.5	2.68	2.32	$0.13 \pm 0.013$	$1.1 \pm 0.1$	2.5–4.6		
PST	1.9	7.4	2.65	2.22	$0.15 \pm 0.014$	$1.2 \pm 0.1$			
EE	1.07	4	1.81	1.37	$0.75 \pm 0.14$	$3.5 \pm 0.5$	~3	3.1	2.36
BTF	1.79	8.4		2.5				2.52	

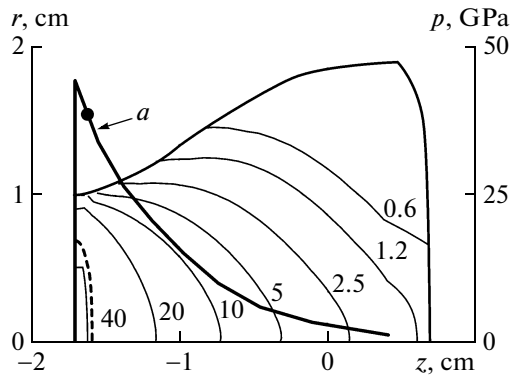


**Fig. 2.** The spatial distribution of the pressure in detonation products of a BTF charge. Solid curves are isobars, the dashed curve is the sonic surface, and curve *a* is the pressure distribution along the charge axis, the dot in which corresponds to the Chapman–Jouguet point.

the Neumann peak and the Chapman–Jouguet plane.

In the case at hand, it was calculated by the ratio  $\frac{\rho_N}{\rho_{cj}}$  and the polytropic exponent  $\gamma$ .

Noteworthy is the systematic discrepancy of the obtained values and, in some cases,  $\Delta$  with the data of [8] (generalizing the results of earlier works of this team of researchers) and a number of other studies. This is due to the fact that our studies were performed with charges of significantly smaller sizes (diameter, length) than those used in other works. In the studies analyzed in [8], it is indicated that the detonation pressure and reaction zone width decrease with decreasing charge diameter, while the Neumann peak excess over the Chapman–Jouguet pressure increases. It is also known that the detonation pressure increases with the charge diameter and during detonation wave propagation. Thus, these disagreements do not contradict the available data, which can be considered as indirect confirmation of the adequacy of the implemented technique.

### DENSITY DISTRIBUTION OF DETONATION PRODUCTS

These studies made it possible to obtain for the first time complete experimental data on the characteristics of the detonation product flow field (density, velocity, pressure) during detonation of cylindrical charges and to separate the sonic surface. In the experiments of this series, the detonating charge was probed in the plane perpendicular to the axis (the experimental design is described in detail in [9]). This makes it possible to obtain information on the dynamics of the distribution of mass in the beam path in a fixed cross section of the detonation flow under study. The axisymmetry of the detonation product flow makes it

possible to reconstruct the density distribution along the radius in the observed charge cross section, based on the data obtained by X-raying at only one angle. Under the assumption of flow stationarity, the total distribution of the detonation product density (the function  $\rho(r, z)$ , where  $r$  and  $z$  are the radial and axial coordinates, is constructed) is reconstructed. In this case, it becomes necessary to solve incorrect inverse problems of dynamic tomography. In the case at hand, it is impossible to apply classical methods based on the Abel inversion [10] due to the nonsmoothness of experimental data and the problems of their regularization.

We developed a novel method for reconstructing the gas-dynamic parameters of the detonation flow by the data on X-ray diffraction experiments. The method is related to a specific problem; however, it makes it possible not only to improve significantly the density reconstruction accuracy [9], but also to determine the other gas-dynamic parameters, i.e., the mass velocity and pressure distributions [11]. The method for reconstructing the fields of the gas-dynamic characteristics of the detonation flow is based on numerical solution of the gas-dynamic problem in the statement corresponding to experimental conditions. It is assumed that detonation products are described by the polytropic equation of state

$$p(\rho) = p_0 \left( \frac{\rho}{\rho_{00}} \right)^{\gamma(\rho)},$$

where  $p_0$ ,  $\rho_{00}$ , and  $\gamma$  are the parameters to be determined. These parameters were found based on the minimizations of the functional of root-mean-square deviations of the calculated and experimentally obtained X-ray “shadows” of the flow under study at separated nodes of the calculation region. The dependence  $\gamma(\rho)$  was approximated by cubic splines. To solve the problem of multidimensional minimization that arises, we used the simplex method described and implemented in [12]. As a result, a complete picture of the flow, i.e., the distribution of all gas-dynamic parameters  $\rho(r, z, t)$ ,  $p(r, z, t)$ , and  $\mathbf{u}(r, z, t)$  ( $\mathbf{u}$  is the velocity vector), is reconstructed.

The results obtained for a benzotrifuroxan (BTF) charge 20 mm in diameter are shown in Figs. 2 and 3. Figure 2 shows the pressure isobars, sonic surface (dashed curve), and the pressure distribution along the charge axis (curve *a* with the indicated sonic point). In Fig. 3, arrows whose length corresponds to the vector magnitude show the velocity field. Formally, it can be considered that the region of the reconstructed flow characteristics also includes the chemical transformation zone, although the process in the latter is in fact nonisobaric, and the state is not thermodynamically equilibrium. In the distributions of the param-

ters along the axis, we can see the region of abruptly decreasing quantities, which can be approximately identified with the chemical transformation zone terminated by the Chapman–Jouguet point, where  $|\mathbf{u}| = c$  ( $c$  is the speed of sound).

An analysis of the technique shows that the spatial and temporal accuracy of the reconstruction of the flow parameters is  $\sim 0.2$  mm and  $\sim 0.2$   $\mu$ s, respectively, and the accuracy of the calculated gas-dynamic characteristics is no worse than 10% on the time scale of 0.5  $\mu$ s. In the energy release region, on the time scale of 0.2  $\mu$ s, the obtained values are estimated. The data obtained allowed us to calculate the unloading adiabat whose polytropic exponent appeared close to the classical value,  $\gamma = 3$ .

### CARBON CONDENSATION IN DETONATION PRODUCTS

This study allowed us to determine for the first time the sizes of the zone in which carbon particles are condensed during detonation of explosives with excess carbon and to describe the dynamics of particle size growth. The idealized model representation of the completion of the exothermic transition of the initial explosive, in general, to the final detonation products in the Chapman–Jouguet plane is subjected to valid criticism when analyzing actual detonation processes and constructing more adequate models of the development of detonation. One of the discussed elements of the detonation transition kinetics is the problem of the role of carbon condensation during detonation of an explosive with a negative oxygen balance and the possibility of continuing condensation behind the Chapman–Jouguet plane. In [13] and a number of other studies, it was shown that the assumption about carbon condensation behind this plane allows more accurate description of the experimental data. To study the carbon condensation process, we used the effect of small-angle deflections of the probe SR beam, caused by density fluctuations of the object under study, i.e., small-angle X-ray scattering. When designing the experiments of this series, the collimated SR beam, as in the previous case, was directed across the explosive charge, and the detector was positioned in parallel to the charge axis. The angular range of small-angle X-ray measurements was  $\sim 4 \times 10^{-4}$ – $10^{-2}$  rad (2–100 detector channels). Such a range allows measurements of small-angle X-ray scattering from particles from  $\sim 2.0$  to  $\sim 75$  nm in size. Each SR pulse fixes the scattering distribution depending on the angle. Pulses recur in 0.5  $\mu$ s, which makes it possible to obtain a “diffraction cinema” of 32 frames each 1 ns long.

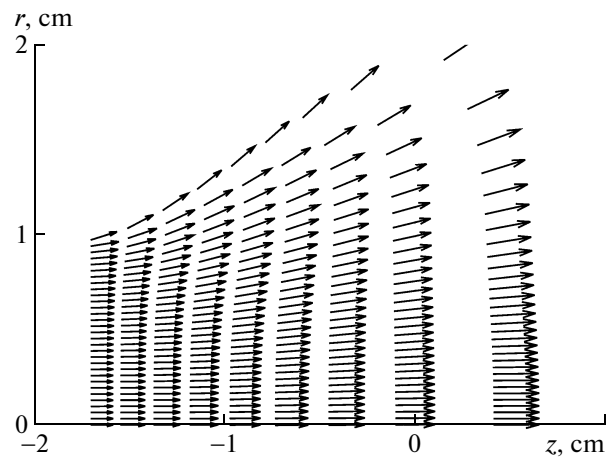


Fig. 3. Velocity field of spreading detonation products of a BTF charge. The arrow length corresponds to the velocity magnitude.

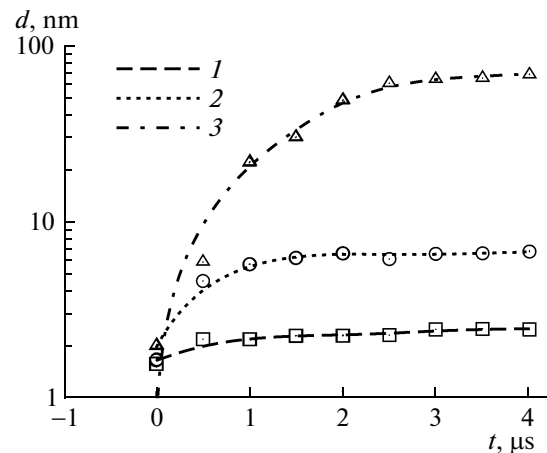


Fig. 4. Growth dynamics of carbon nanoparticles: (1) TATB, (2) TH50/50, (3) BTF.

Detonation of pressed trotyl, hexogen, the TH50/50 mixture, BTF, and TATB-based mixture charges 30–32 mm long and 20 mm in diameter was studied. Initiation was conducted through an intermediate charge based on plasticized pentaerythrite tetranitrate (PETN). The results were interpreted using conventional techniques [14]. A detailed analysis of the results of the study allows the conclusion that free carbon condensation lasts  $\sim 1$ – $2$   $\mu$ s, which substantially exceeds the duration of the chemical reaction zone, estimated by various methods. In this case, it is complicated to separate the particle formation dynamics in the diamondlike phase. Data processing according to [14] allows us to estimate the dynamics of sizes of condensed carbon nanoparticles (Fig. 4). We can see that nanoparticles of size  $d \sim 2$  nm are fixed at the detonation front. Then the particle size increases

and reaches  $d \sim 2.5\text{--}3.0$ ,  $\sim 5\text{--}6$ , and  $60\text{--}70$  nm for TATB, TH50/50, and BTF, respectively, in  $t = 2\text{--}3$   $\mu\text{s}$ . Figure 4 shows the capability range of the technique.

The final sizes determined in dynamic experiments are almost identical to the values obtained in the study of retained explosion products [15].

Thus, implementation of the techniques based on the use of SR as a probe beam offered new possibilities of studying the detonation processes in condensed explosives. In the case of stationary detonation, it became possible to measure the density distribution in the detonation wave front and spreading products. The experimental data obtained made it possible to reconstruct the total fields of the distributions of all gas-dynamic parameters of the detonation process in space and time. This offers new opportunities for verifying the existing equations of state and constructing new equations of state of explosives and detonation products, and the detonation transformation kinetics. In the latter case, the results obtained using the effect of small-angle scattering are essential.

#### ACKNOWLEDGMENTS

This study performed using the equipment of the Shared Service Center of the Siberian Synchrotron and Terahertz Radiation Center was supported by the Russian Foundation for Basic Research (project nos. 12-01-00177-a and 11-03-00874-a), the Ministry of Education and Science of Russia, and the Siberian Branch of the Russian Academy of Science (integration project no. 65).

#### REFERENCES

1. G. I. Kulipanov and A. N. Skriniskii, *Usp. Fiz. Nauk* **122**, 369 (1977).
2. G. V. Fetisov, *Synchrotron Radiation. Methods for Studying the Material Structure* (Fizmatlit, Moscow, 2007) [in Russian].
3. A. N. Aleshaev, P. I. Zubkov, G. N. Kulipanov, et al., *Fiz. Goreniya Vzryva* **37** (5), 104 (2001).
4. V. M. Aul'chenko, O. V. Evdokov, I. L. Zhogin, et al., *Prib. Tekh. Eksp. No. 3*, 20 (2010) [*Instrum. Exp. Tech.* **53**, 334 (2010)].
5. K. A. Ten, O. V. Evdokov, I. L. Zhogin, et al., *Fiz. Goreniya Vzryva* **43** (2), 91 (2007).
6. B. G. Loboiko and S. N. Lyubyatinskii, *Fiz. Goreniya Vzryva* **36** (6), 45 (2000).
7. A. N. Dremin, S. D. Savrov, V. S. Trofimov, and K. K. Shvedov, *Detonation Waves in Condensed Media* (Nauka, Moscow, 1970) [in Russian].
8. A. V. Fedorov, A. L. Mikhailov, L. K. Antonyuk, et al., *Fiz. Goreniya Vzryva*, No. 3, 62 (2012).
9. E. R. Prueel, L. A. Merzhievskii, K. A. Ten, et al., *Fiz. Goreniya Vzryva*, No. 3, 121 (2007).
10. V. V. Pikalov and N. G. Preobrazhenskii, *Reconstruction Tomography in Gas Dynamics and Plasma Physics* (Nauka, Novosibirsk, 1987) [in Russian].
11. K. A. Ten, E. R. Prueel, L. Merzhievsky, et al., *Nucl. Instrum. Methods Phys. Res. A* **603**, 160 (2009).
12. [www.gnu.org/software/gsl](http://www.gnu.org/software/gsl)
13. C. M. Tarver, J. W. Kury, and R. D. Breithaupt, *J. Appl. Phys.* **82**, 3771 (1997).
14. D. I. Svergun and L. A. Feigin, *Small-Angle X-Ray and Neutron Scattering* (Nauka, Moscow, 1986) [in Russian].
15. V. M. Titov, V. F. Anisichkin, and I. Yu. Mal'kov, *Fiz. Goreniya Vzryva* **35** (3), 117 (1989).